Natural Hazards
https://doi.org/10.1007/s11069-024-06927-0

ORIGINAL PAPER

Tree rings reveal the correlation between the Kaindy Lake submerged forest and the historical 1889 M 8.2 Chilik earthquake (Kazakhstan)

Cécile Miramont[1] · Magali Rizza[2,7] · Frédéric Guibal[1] · Elodie Brisset[1] · Lenka Brousset[1] · Frédéric Guiter[1] · Paul Millagou[1] · Satbek Sarzhanov[3] · Baurzhan Adilkhan[3] · Ünal Akkemik[4] · Kuralay Mazarzhanova[5] · Arailym Kopabayev[5] · Aidyn Mukambayev[6]

Received: 19 May 2024 / Accepted: 13 September 2024

Abstract

Paleoseismic studies are essential to improve earthquake hazard mitigation, a challenging task in the Tian Shan mountains characterized by numerous active faults, frequent strong earthquakes, and abundant triggered landslides. Here, we date the debated formation of Kaindy Lake, the famous landslide-dammed lake in southeastern Kazakhstan, included in the UNESCO World Network of Biosphere Reserves. Our dendrochronological study compares ring-width patterns from dead trees (*Picea schrenkiana*) still standing in the lake with living trees growing on surrounding slopes and other trees on the landslide debris. Our results place the formation of the lake to just after 1888 A.D. (the last ring of sunken trees) and before 1898 A.D. (the first established trees on the landslide), a period for which only the 1889 A.D. Chilik earthquake (M 8.2) has been reported and caused extensive damages in the region (surface ruptures, landslides). Thus, we propose that the landslide was triggered during this historical earthquake, questioning the previously preferred date of 1911 A.D., and the local common belief. Furthermore, our results indirectly complement previous paleoseismic studies at 8.5 km away, for which the most recent event in the region was poorly defined by geochronological dating, but suggested a surface rupture associated with the 1889 A.D. earthquake. The proximity of the landslide to the surface rupture would place it in the epicentral zone of the Chilik earthquake.

Keywords Dendrogeomorphology · Tree ring · Dammed lake · Sunken forest · Landslide · Earthquake

1 Introduction

The Tian Shan mountain range in Central Asia accommodates a large part of the shortening between Eurasia and India plates (Tapponnier and Molnar 1979), with strong earthquakes recorded in historical and instrumental catalogs (Kalmetieva et al. 2009). This mountain range is also characterized by numerous large rock slope failures, often blocking major

Extended author information available on the last page of the article

Published online: 04 October 2024

rivers, and creating dammed lakes (Havenith et al. 2003; Strom and Abdrakhmatov 2018). Most of these extensive slope failures are located on or near active faults and their spatial clustering is often correlated with seismic activity in the Tien Shan (Strom and Korup 2006), supporting the hypothesis that strong earthquakes have triggered most of these landslides (Delvaux et al. 2001; Havenith and al. 2003; Strom and Abdrakhmatov 2018). Therefore, landslides and rock avalanches can be considered as indirect evidence to date prehistoric earthquakes, but we cannot exclude the possibility of multiple superimposed deposits resulting from re-activations at the same site.

At the foot of the Zailisky Alatau, the northernmost mountain range of the Tien Shan, Almaty is one of Kazakhstan's largest and fastest-growing cities with about 2 millions inhabitants. In this region, although much of the instrumentally recorded seismicity has been moderate in size (Sloan et al. 2011), significant seismic hazard and risks are identified for Almaty City (Amey et al. 2021). Indeed, a remarkable series of large historical earthquakes (Fig. 1a) struck the Zailisky-Kungey Range area from 1885 A.D. to 1978 A.D. and caused significant material damages, human losses, and numerous slope failures and surface ruptures (Hay 1888; Mushketov 1891; Bogdanovitch et al. 1914; Delvaux et al. 2001; Abdrakhmatov et al. 2016; Arrowsmith et al. 2017). Many questions remain about the mapping and the timing of the surface ruptures associated with these earthquakes, which took place in sparsely populated and mountainous regions. To improve earthquake hazard mitigation plans in this region, paleoseismological studies have been conducted to determine the ages of surface-rupturing events or recurrence times (Abdrakhmatov et al. 2016; Arrowsmith et al. 2017; Deev et al. 2016). However, geochronological dating methods (radiocarbon or luminescence dating) used to bracket the ages of past earthquakes in paleoseismic trenches have too broad temporal uncertainties that prevent us from discriminating between closely timed historical earthquakes.

Our study focuses on a landslide that blocked the river Kaindy and created Lake Kaindy, one of the most visited tourist sites in Kazakhstan (Figs. 1b, 2). The highlight of the lake is the remains of dozens of spruce trees (*Picea schrenkiana* Fisch. & C.A.Mey.) rising out of its turquoise water (Fig. 3). The literature associated with the Kaindy dammed-lake is sparse and some contradictory information are written about the origin and timing of the landslide. First of all, there is a common confusion between the dammed Lake Kaindy, in which flows the River Kaindy (SE Kazakhstan, 42.986° N 78.465° E, Озеро Каинды, the topic of this paper), and the Kaindi landslide located at 42.718° N 76.205° E near the village of Kaindi (Кайинды, Kyrgyzstan, see location in Fig. 1a), formed after the 1911 Kemin earthquake (Bogdanovich et al. 1914; Delvaux et al. 2001; Strom and Abdrakhmatov 2018). Moreover, no absolute dating of the Kaindy landslide that created the lake is currently available. It is expected that most recent rockslides in the study area could have been triggered by the historical 1889 Chilik or the 1911 Kemin earthquakes (Strom and Abdrakmatov 2018). Indeed, the landslide proximity to the fault segments inferred for the 1889 earthquake may suggest a seismic origin (Abdrakhmatov et al. 2016; Strom and Abdrakhmatov 2018). Nevertheless, it has long been believed (National Park brochure, Wikipedia, local lore, Guo 2019, Камендровская et Романова 2021, Виноградов 2017) that Lake Kaindy was created by the 1911 Kemin earthquake but without any scientific evidence. A first dendrological study has been carried out by Akkemik et al. (2022), but the results are under discussion and a larger sampling size appears necessary to resolve the age of the lake formation. Last, samples of submerged trees of the Kaindy lake collected by V.A. Gapich resulted in radiocarbon ages of 430 ± 60 BP (1406–1635 cal. A.D., 2σ), indicating that the timing of the lake that drowned the spruce forest could be much older (Strom and Abdrakhmatov 2018).

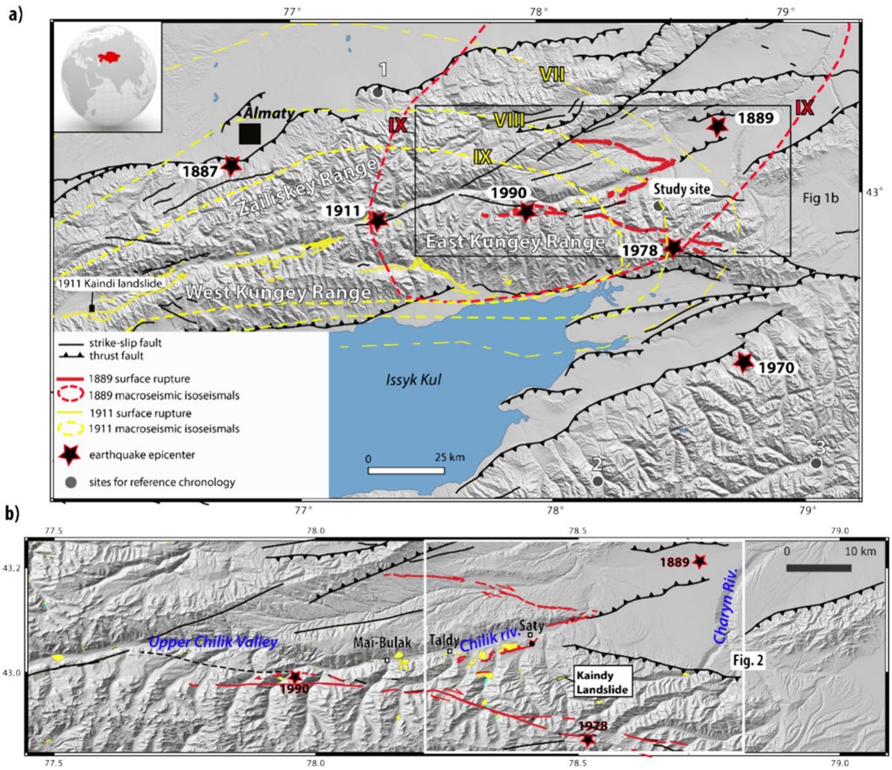

Fig. 1 **a** Macroseismic maps of the 1889 and 1911 earthquakes in the Kungey range. The stars represent the epicenters for selected earthquakes with M > 6.5. The 1889 and 1911 surface ruptures (Abdrakhmatov et al. 2016; Arrowsmith et al. 2017) are represented in color. Isoseismal lines are represented in MSK-64 scale (Januzakov et al. 2003; Bindi et al. 2014). Three of the selected dendrochronological sites for reference chronologies are Solomina-Ulken (1), Schweingruber—Tschongkys (2), and Solomina—Koeliu (3). Data can be found at https://www.ncei.noaa.gov/access/paleo-search; **b** Active faults and landslides between the upper Chilik Valley and the Charyn River. The active faults are in black and the trace for the 1889 surface rupture is in red (after Abrakhmatov et al. 2016). Stars are epicenters of large earthquakes. Areas of land-sliding are reported in yellow after Bogdanovitch et al. (1914) and Havenith et al. (2003). Location of Abra-khmatov et al.'s (2016) trench is located by the black dot close to Saty city. The white box locates Fig. 2

To resolve the debated issue of the timing of the Kaindy dammed-lake, we propose to apply a dendrochronological approach by collecting tree-ring samples from the sunken trees and living trees growing on surrounding slopes. Tree rings are among the most accurate paleoenvironmental archives and dendrochronology is the only known method (with varves analyses) that provides annual or seasonal accuracy of past environmental disturbances (Speer 2010). Moreover, tree rings analysis is a powerful tool to date geomorphic events as landslides, particularly in remote and sparsely populated areas whose history is not well documented (Alestalo 1971; DeGraff and Agard 1984; Cook and Kairiukstis 1990; Stoffel and Bollschweiler 2008; Black et al. 2023).

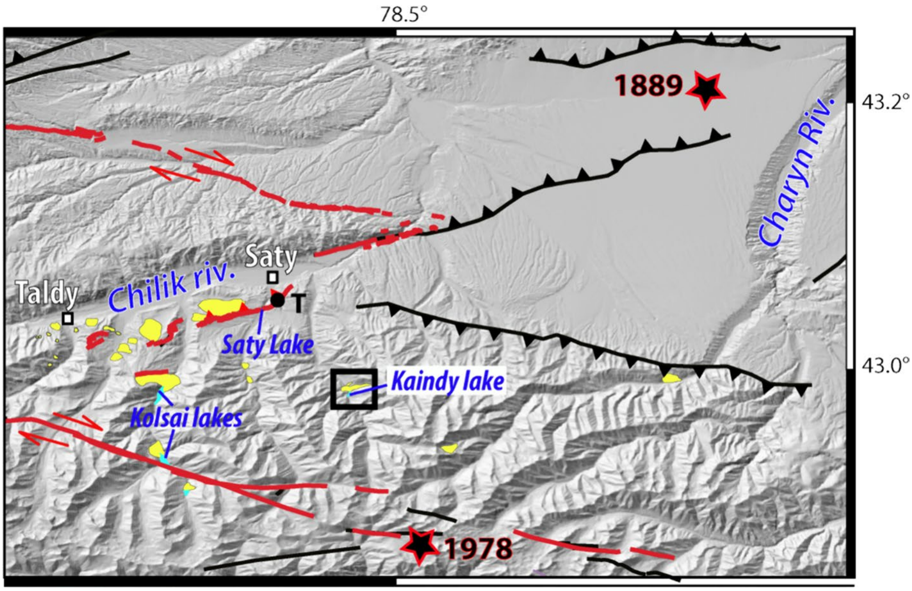

Fig. 2 Active faults and landslides. The active faults are in black and the trace for the 1889 surface rupture is in red (after Abrakhmatov et al. 2016). Stars are epicenters of large earthquakes. Areas of landsliding are reported in yellow after Bogdanovitch et al. (1914) and Havenith et al. (2003). Location of Abrakhmatov et al.'s (2016) trench is located by the black dot close and T. The black box locates our study area and Fig. 5

2 State of the art

2.1 A remarkable cluster of large earthquakes struck the eastern Kungey range

Our study area is located on the eastern part of the Kungey range (Fig. 1a) struck by a cluster of large earthquakes (M > 6.5) in 1887 (Verny), 1889 (Chilik), 1911 (Kemin) and 1978 (Dzhalanash-Tyup). The June 8, 1887 Verny earthquake (M7.3), with an epicenter located at only ~ 30 km from Almaty, has caused widespread landsliding within the loess deposits of the range front (Hay 1888) but no surface ruptures have been yet identified (Tatevossian 2007). Two years later, the Chilik earthquake occurred on 11 July, 1889 (M8.2) causing destructions in a wide region centered between the Charyn and Chilik Rivers (Fig. 1a, b), where the most intense damage was reported (Mushketov 1891; Bindi et al. 2014; Kulikova and Krüger 2015). The maximum local intensities reached up to intensity X from Rossi–Forel scale (Mushketov 1891) to intensity IX on the MSK-64 scale (Januzakov et al. 2003; Bindi et al. 2014). Information about this earthquake came from questionnaires filled out by earthquake witnesses and the observations are sparse. No surface ruptures were reported in 1889 but observations of fissures or numerous landslides were later reported (Bogdanovitch et al. 1914). More recently, Tibaldi et al. (1997) and Abdrakhmatov et al. (2016) mapped more than 175 km of fresh fault scarps on a Z-shape (Figs. 1, 2), with conjugate oblique left-lateral and right-lateral slip on three separate fault patches, and step overs of several kilometers between them. Detailed surveys on the ~ 30 km Saty segment (Fig. 2), located only 8.5 km from our study site, revealed fresh surface ruptures in the morphology, involving co-seismic slip of up to 10 m (Abdrakhmatov

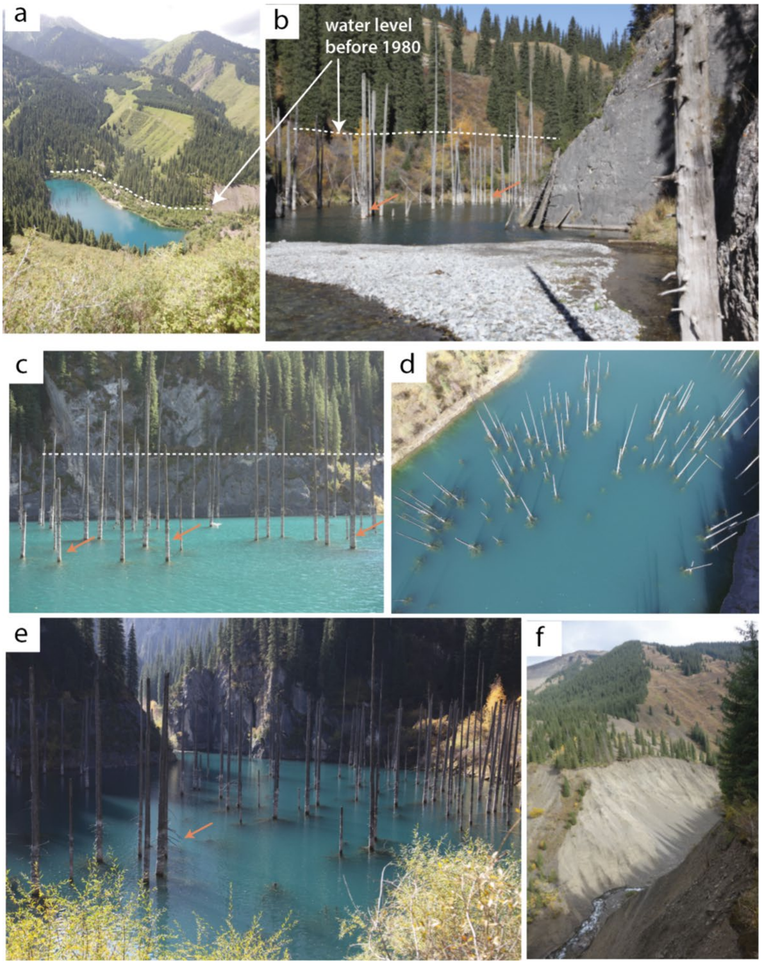

Fig. 3 Photographic panels of Kaindy Lake. The dashed white line is for the water level before 1980. **a** Overview of Kaindy Lake from the North-East.; **b** and **c** Sunken trees (*Picea Skrenkania*). The white hue and remains of lateral branches (orange arrow) show the ongoing level dropping **d** and **e** Drowned snags extending above the surface of the lake with remaining submerged branches **f** Erosional canyon of the Kaindy River in the landslide toe

et al. 2016). Along this scarp, paleoseismic investigations (noted T in Fig. 1b) found that this topographic scarp was likely formed during a single earthquake, dated to be younger than 1342 ± 56 A.D., and the only one for at least 5000 years. As no other large historical earthquakes are reported in the Chilik region, it has been proposed that the Saty fault segment (Fig. 2) probably formed during the 1889 Chilik earthquake, although this is not certain (Abdrakhmatov et al. 2016). The Kemin earthquake occurred on 3rd January, 1911 (M7.8–8.0, Fig. 1), with local maximum intensities reported to VIII on the MSK-64 scale in the Chilik-Saty area, where is located our study site (Januzakov et al. 2003; Bindi et al. 2014). Detailed descriptions of surface effects were investigated a few months after, during spring 1911 by Bogdanovich et al. (1914). This field survey allowed a unique map of primary and secondary surface deformation and mass movements associated with the Kemin earthquake (Fig. 1). It was to be noticed, that this earthquake caused numerous large-scale landslides, which killed many people in the Kungey region (Bogdanovich et al. 1914; Delvaux et al. 2001). Other reconnaissance mappings of the rupture associated with the Kemin earthquake have been recently performed and this earthquake produced a total of 155–195 km of rupture (Fig. 1) on different fault patches running on the western part of the Kungey Range and on the southern slope of the eastern Kungey range (Delvaux et al. 2001; Arrowsmith et al. 2017). The 1978 Dzhalanash-Tyup earthquake (M6.9) has an epicenter located in the Kungey range (Kulikova and Krüger 2015), with maximum intensities reported to be VIII on the MSK-64 scale at our study site (Januzakov et al. 2003; Bindi et al. 2014), but no surface ruptures have been yet recognized. Two other earthquakes with moderate magnitude were also recorded in this region on 5 June 1970 (M6.3), and on 12 November 1990 (*M*6.3) (Januzakov et al. 2003).

2.2 Landslides in the Chilik area

Large landslides were triggered in the Chilik valley by both the 1889 and 1911 earthquakes (Fig. 1b). For the upper western part of the Chilik valley, Bogdanovitch et al. (1914) reported some effects associated with the 1889 earthquake in the Chilik valley, but this area was also strongly affected by intensive rock-falling and mass movements during the 1911 Kemin earthquake. For example, at Mai-Bulak a part of a hillside collapsed into the Chilik valley and blocked the channel of the river, but the dam was washed away only in three days. In the Taldy area, many collapsed rocks were observed in 1911 but at the same place, where larger deformations occurred in 1889, according to local people. Evidence of the 1889 earthquake is reported in the Saty valley where two rock falls dammed the river channel and formed a small lake still visible (labelled Saty lake in Fig. 2). It is interesting to note that along or close to the Saty fault trace mapped by Abdrakhmatov et al. (2016), numerous large slope failures are also reported, and are sometimes associated with dammed lakes on the Kolsai valley (Fig. 2), also called Kul-su (Havenith et al. 2003; Strom and Abdrakhmatov 2018). These prehistoric landslides are of unknown age and given their vicinity to active faults, they were probably triggered by earthquakes. Along the Kaindy valley, which has not been surveyed by Bogdanovich et al. (1914), is standing one of the famous dam lakes of this region: the Kaindy lake.

2.3 The landslide-dammed Lake Kaindy

Lake Kaindy is a landslide-dammed lake located at 1867 m a.s.l in the Kaindy River valley (42.984853° N, 78.465738° E, Fig. 1b) of 445-m-long, 100-m-wide and around 30-m-deep (Fig. 3). The lake catchment area covers ~ 50 km^2 and includes several peaks that culminate at 3790 m a.s.l. The lake is surrounded by rocky slopes and cliffs covered by *Picea schrenkiana* trees until 2900 m a.s.l. Many trees (*Picea schrenkiana*) have been planted during the twentieth century. The words "Kaindy, Kaindi, Qaiyndy or Kaiyndy" means "like a Birch" or "birchen" in Kazakh. It most certainly corresponds to the riparian forest along the river.

The rockslide that formed the Kaindy Lake originated at the upper part of the right slope of the valley (Fig. 4), has an estimated volume of 8 millions m^3, and blocks the river course (Strom and Abdrakhmatov 2018). Several scars are visible in the upper part of the slope, and we noted several bodies more or less vegetated within the

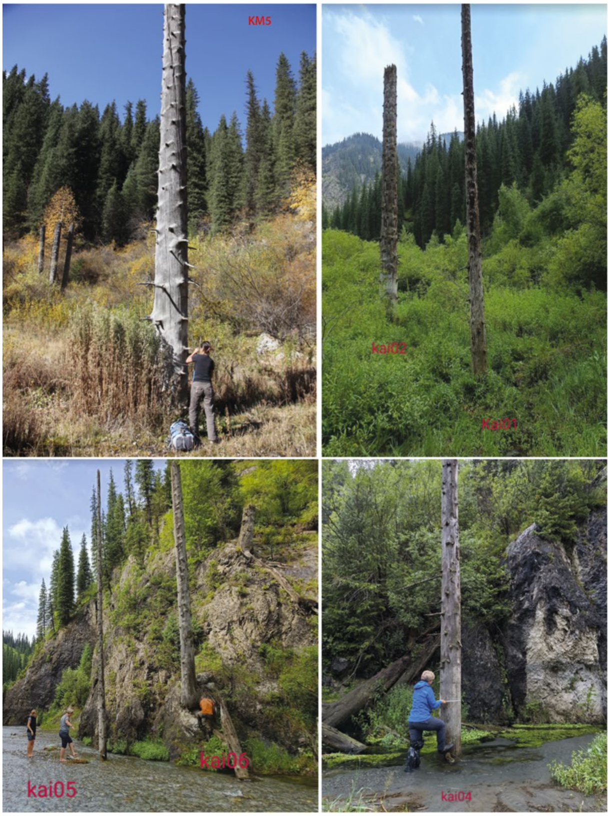

Fig. 4 Field sampling of dead trees around Lake Kaindy

landslide, which may reflect different reactivation phases (Fig. 4). A secondary smaller landslide is mapped a hundred meters downstream of the major landslide-dam.

The trees (*Picea schrenkiana*) that grew upstream of the dam were drowned still standing, forming a unique underwater forest (Fig. 3). Local people call them « guardians of the lake» and compare them to masts of submerged ships. The upper part of the boles protruding from the surface of the lake turned white and they lost their branches. Clear water allows us to see deep down inside the lake: the algae and other aquatic plants that cover submerged branches create the visual impression that dead trees still have needles. Because of the cold water of the lake (maximal temperature does not exceed 6° C in summer), the sunken trees are perfectly preserved.

In 1980, the dam was partially breached, and the lake level dropped by about 10 m (Strom and Abdrakhmatov 2018). A deep erosional canyon was formed, and traces of this outburst flood are visible more than 2.5 km downstream. The former high level is easily visible on satellite images from 1976 (white line in Fig. 4) and today in the surrounding morphology as young plants have colonized the base of the slope (Figs. 3c, 4). Since then, the level of the lake kept dropping, corresponding to the white hue on the sunken trunks. The near-perfect preservation of the underwater lateral branches shows that the water level has never been lower than today.

2.4 Environmental setting

Kaindy Lake, part of the Kolsai National Park, which is home to many rare and endangered species and unique natural features, was included in UNESCO's world network of Biosphere Reserves in 2021 to preserve its remarkable lakes, rich biodiversity, and historical and cultural heritage. The local continental climate is classified as a Dfc climate according to the Köppen climate classification (Peel et al. 2007), and is affected by elevation and exposure differences. According to the nearest meteorological station of Asy (43.225109° N, 77.871907° E), the annual mean precipitation is above 400 mm occurring both as snow and rainfall mainly from May to August. The long-term mean annual air temperature is about 0.5 °C, with January and July averaging about − 13 °C and 12 °C, respectively (Russian Meteorological Agency 2023).

3 Dendrochronology method and sampling strategy

Dendrochronology is a widely recognized tool for dating past earthquake events and seismic-induced geomorphic processes such as landslides (Sheppard and Jacoby 1989; Speer 2010; Bekker 2010; Owczarek et al. 2017; Jacoby et al. 1988, 1997; Dziak et al. 2021). Counting and crossdating tree rings, and analyzing growth patterns can provide valuable information about the timing, frequency, and magnitude of such extreme natural events. During an earthquake, trees can be directly impacted by ground acceleration shaking their roots, causing mortality and growth ring disturbance (reaction wood in tilted trees, narrow or missing ring during the years following the event). Tree-ring analysis is also a valuable way to identify earthquakes by examining the effects of seismologically-induced landslides (Carrara and O'Neill 2003, 2010). In particular, tree-ring analyses have been successfully used to date sunken forests drowned in landslide-dammed lakes triggered by earthquakes. The most famous example is the earthquake that happened in the Cascadia Subduction Zone (Pacific Northwest coast of the USA), which caused a tsunami that hit the coasts of Japan. The timing of the earthquake has been constrained to the winter of 1699/1700 A.D. by dating the outermost growth rings of Douglas fir of «ghost forests» drowned by the tsunami inundation (Atwater et al. 2005; Atwater and Yamaguchi 1991; Yamaguchi et al. 1997). In the coastal regions of Oregon and Washington states characterized by widespread slope instability, many studies using tree-ring analyses of sunken trees were performed successfully to date numerous earthquakes and landslide-dammed lakes from historical times (Jacoby et al. 1992, 1997; Struble et al. 2020, 2021). Moreover, the ages of the trees themselves supply important information to date geomorphic events. Specifically, the age of the oldest trees growing on a landslide can be used to estimate the minimum age of the landslide (Lawrence 1936, 1937).

In this study, we attempt to date the landslide and the Kaindy lake formation by comparing ring-width patterns from dead sunken trees with nearby living trees. In this aim, 32 dead trees from the sunken forest were sampled to assess the date of their outer preserved rings. Ideally, it would have been preferable to dive into the lake to collect samples with bark, but this was not possible due to logistical constraints. We sampled the previously sunken dead trees located around the lake, which are today easily accessible due to the drop in water level in 1980 (Fig. 3). The bark was visible at the base of one trunk (KM2) and we sampled it one meter above this point. Generally speaking, the wood showed little signs of degradation. Nine trees were still in living position (Fig. 4) and 13 were lying. To build a local reference chronology, 19 living trees were sampled on the surrounding slopes, both on the right and left sides of the river. Moreover, to investigate the age of the last activation phase of the landslide, 18 living trees were sampled on the active part of the landslide (Tables 1, 2 and Fig. 5). Our sampling strategy complements another sampling campaign conducted by Akkemik et al. (2022), in which 9 dead trees and 13 living trees were also analyzed. These 13 living trees were sampled from the west slope (its aspect is east) of the lake. They were from the opposite side of the landslide and above the lake and far from the flood effect. This paper will discuss the interpretations of the collected data taken as a whole.

When it was possible, two increment cores were collected on each tree using an increment borer (diameter 5.15 mm) to overcome ring-width variation around the tree (Grissino-Mayer 2003). Marks of sampling were filled with wood dowels, so we did not jeopardize the integrity of this touristic place. All samples were air-dried, glued to mounts, and polished using progressively finer sandpaper up to 400 grain size to clearly see the tree-ring limits. Afterward, wood cores were digitized using a resolution of 1200 dpi. Ring-widths (TRW) were measured using both the software CooRecorder® (Maxwell and Larsson 2021) and a LINTAB® measuring system with a precision of 0.01 mm. Standard dendrochronological techniques were employed in chronology development. Cross-dating analyses were performed using the TSAPWin® software (Rinn 1991–2023). All chronologies were built by using standard statistical tests and visual comparison of the raw TRW curves: the coefficient of coincidence or *Gleichläufigkeit* [Glk] (Eckstein and Bauch 1969), the Student *t* values obtained with Baillie and Pilcher indices (Baillie and Pilcher 1973) and Hollstein indices (Hollstein 1980). We also used the crossdate index (CDI) provided by TSAP software (combining *t* values and *Gleichläufigkeit*) which is a powerful tool in crossdating (Rinn 1991–2023). Typically, Glk values above 60%, t-values above 3.5 and DCI above 30 are considered statistically robust (Baillie and Pilcher 1973; Hollstein 1980), providing confidence in the crossdating results. Overall, crossdating and measuring errors were checked with the COFECHA software (Holmes 1983). We estimated the establishment date for each living tree by adding 10 years to the age of the pith as the cores were extracted from trees at 1.2 m high. When inner rings were missing in the core samples, we estimated the distance to pith (in years) with the tool available in CooRecorder®. This tool is based on the curvature of tree-ring boundaries and the average width of internal rings (Maxwell and Larsson 2021; Pirie et al. 2015).

4 Dendrochronology: results

Taken together [this sampling campaign and previous Akkemik study (Table 1)], the living trees provided a reference chronology of 205 years (namely “KAILife”, blue record in Figs. 6, 7a) spanning 1818 A.D. to 2022 A.D. with high values for statistical tests (Glk > 60, tvBP > 5, tvH > 5, CDI > 30). 27 individual chronologies from the dead trees crossdated were included in a mean chronology labeled “KAIDead” (red record, Figs. 6, 7a), spanning 1717 A.D. to 1888 A.D. with significant values for statistical tests (Glk > 67, tvBP > 6.7, tvH > 6.4, CDI > 45 when OVL > 80) Table 2 and Supplementary Information). 2 dead trees (KAI8 and KM9) with only 31 and 54 rings, respectively, could not be crossdated. 3 lying trees (KAI07, KAI15 and KAI19) do not match with the other dead trees but crossdate with KAILife, attesting that they fell down recently.

Table 1 Kaindy living trees

	Sampling date	Tree label	Circumference (cm)	GPS LAT	GPS LONG	Position	Tree-ring serie		Number of rings between the pith and the start of the tree-ring serie (estimation)	Germination date (estimation)	Lifetime (estimation) years
							Date begin	Date end			
1	08-07-2022	KV02 AB	205	42.991264	78.471322	Landslide surface (right side)	1958	2022	46	1902	120
2	08-07-2022	KV04 A	187	42.991657	78.471318	Landslide surface (right side)	1939	2022	1	1928	94
3	08-07-2022	KV06 A	251	42.991405	78.472223	Landslide surface (right side)	1933	2022	1	1922	100
4	08-07-2022	KV08 A	167	42.991202	78.473589	Landslide surface (right side)	1931	2022	1	1920	102
5	08-07-2022	X01 AB	140	42.98981	78.47073	Landslide surface (right side)	1947	2022	2	1935	87
6	08-07-2022	X02 AB	139	42.989626	78.470574	Landslide surface (right side)	1943	2022	3	1933	89
7	08-07-2022	X03 AB	137	42.989414	78.470649	Landslide surface (right side)	1922	2022	2	1910	112
8	08-07-2022	X04 AB	231	42.989824	78.47169	Landslide surface (right side)	1913	2022	2	1901	121

Table 1 (continued)

	Sampling date	Tree label	Circumference (cm)	GPS LAT	GPS LONG	Position	Tree-ring serie		Number of rings between the pith and the start of the tree-ring serie (estimation)	Germination date (estimation)	Lifetime (estimation) years
							Date begin	Date end			
9	08-07-2022	X05 AB	186	42.989929	78.472127	Landslide surface (right side)	1925	2022	1	1914	108
10	08-07-2022	X06 AB	186	42.989643	78.472622	Landslide surface (right side)	1929	2022	2	1917	105
11	08-07-2022	X07 AB	210	42.990047	78.473497	Landslide surface (right side)	1933	2022	2	1921	101
12	08-07-2022	X08 AB	170	42.989419	78.473157	Landslide surface (right side)	1932	2022	2	1920	102
13	08-07-2022	KV15 A	188	42.989830	78.468468	Landslide surface (right side)	1942	2022	–	–	140
14	08-07-2022	KV17 A	206	42.989797	78.468287	Landslide surface (right side)	1942	2022	2	1930	92
15	08-07-2022	KV19 A	219	42.989680	78.468512	Landslide surface (right side)	1922	2022	2	1910	112
16	08-07-2022	KV21 AB	203	42.987953	78.465503	Landslide surface (right side)	1935	2022	27	1898	124

Table 1 (continued)

	Sampling date	Tree label	Circumference (cm)	GPS LAT	GPS LONG	Position	Tree-ring serie		Number of rings between the pith and the start of the tree-ring serie (estimation)	Germination date (estimation)	Lifetime (estimation) years
							Date begin	Date end			
17	08-07-2022	KV23 AB	178	42.987872	78.465580	Landslide surface (right side)	1947	2022	2	1935	87
18	08-07-2022	KV25 AB	228	42.987661	78.466069	Landslide surface (right side)	1928	2022	0	1918	
19	07-07-2022	KV01 AB	198	42.980413	78.465469	Slope (left side)	1973	2022	70	1893	129
20	09-07-2022	KV26 A	166	42.98589	78.46384	Slope (left side)	1931	2022	1	1920	102
21	09-07-2022	KV27 A	163	42.98588	78.46349	Slope (left side)	1932	2022	1	1921	101
22	09-07-2022	KV28 A	176	42.98567	78.46375	Slope (left side)	1926	2022	15	1901	121
23	09-07-2022	KV29 A	210	42.98355	78.46354	Slope (left side)	1950	2022	77	1863	160
24	09-07-2022	KV30 A	241	42.98175	78.463826	Slope (left side)		2022			
25	09-07-2022	KV31A	267	42.97854	78.46624	Slope (left side)	1931	2022	–		
26	Oct-15	KV1 2015 A	No data	42.982911°	78.463525°	Slope (left side)	1918	2015	2	1906	109
27	Oct-15	KV2 2015 A	No data			Slope (left side)	1920	2015	2	1908	107
28	Oct-15	KV3 2015 A	No data			Slope (left side)	1926	2015	2	1914	101
29	Oct-15	KV4 2015 A	No data			Slope (left side)	1935	2015	–		
30	Oct-15	KV5 2015 A	No data			Slope (left side)	1860	2015	–		
31	Oct-15	KV6 2015 A	No data			Slope (left side)	1944	2015	2	1932	83
32	08-07-2022	KV03 AB	246	42.987430	78.470541	Slope (right side)	1942	2022	106	1826	196
33	08-07-2022	KV05 AB	196	42.987202	78.470240	Slope (right side)	1911	2022	71	1830	192

Table 1 (continued)

	Sampling date	Tree label	Circumference (cm)	GPS LAT	GPS LONG	Position	Tree-ring serie		Number of rings between the pith and the start of the tree-ring serie (estimation)	Germination date (estimation)	Lifetime (estimation) years
							Date begin	Date end			
34	08-07-2022	KV07 A	232	42.987271	78.470205	Slope (right side)	1894	2022	2	1882	140
35	08-07-2022	KV09 AB	152	42.987707	78.470649	Slope (right side)	1915	2022	29	1876	146
36	08-07-2022	KV11 AB	128	42.988044	78.470681	Slope (right side)	1917	2022	2	1905	117
37	08-07-2022	KV13 A	194	42.988248	78.471074	Slope (right side)	1917	2022	2	1905	117
Trees sampled by Akkemik et al (2022)											
1	12-07-2022	KAY08A	207	42.985015°	78.465873°	Slope (left side)	1866	2022	16	1840	182
2	12-07-2022	KAY10A	154			Slope (left side)	1818	2022	0	1812	214
3	12-07-2022	KAY11AB	155			Slope (left side)	1891	2022	1	1880	142
4	12-07-2022	KAY12AB	113			Slope (left side)	1863	2022	0	1858	169
5	12-07-2022	KAY13AB	214			Slope (left side)	1872	2022	0	1865	160
6	12-07-2022	KAY14A	205			Slope (left side)	1882	2022	0	1874	150
7	12-07-2022	KAY15A	182			Slope (left side)	1905	2022	0	1895	127
8	12-07-2022	KAY16A	164			Slope (left side)	1824	2022	4	1810	212
9	12-07-2022	KAY17A	151			Slope (left side)	1897	2022	50	1837	185
10	12-07-2022	KAY18A	171			Slope (left side)	1849	2022	0	1840	183
11	12-07-2022	KAY03A	108			Slope (left side)	1916	2022	0	1908	116
12	12-07-2022	KAY06A	195			Slope (left side)	1880	2022	15	1855	167
13	12-07-2022	KAY7AB	182			Slope (left side)	1890	2022	17	1863	159

Trees with two cores are labeled ’AB’ and those with one core are labeled ’A’

Table 2 Dating results of the sunken trees

	Sampling date	Tree label	Circumference (cm)	GPS LAT	GPS LONG	Position	Tree-ring serie		Number of rings between the pith and the start of the tree-ring serie (estimation)	Germination date (estimation)	Lifetime (estimation) yesrs	Remark
							Date begin	Date end				
1	07-07-2022	KAI01 AB	77	42.981731	78.464153	In situ, erected	1805	**1882**	1	1794	95	
2	07-07-2022	KAI02 AB	225	42.981648	78.464997	In situ, erected	1742	**1886**	29	1703	186	
3	07-07-2022	KAI03 AB	158	42.982863	78.464990	In situ, erected	1746	**1878**	6	1730	159	
4	07-07-2022	KAI04 AB	185	42.981789	78.465387	In situ, erected	1829	**1884**	29	1790	99	
5	07-07-2022	KAI05 A	77	42.983095	78.465042	In situ, erected	1734	**1878**	21	1703	186	
6	07-07-2022	KAI06 A	146	42.983133	78.465143	In situ, erected	1816	**1879**	71	1735	154	
7	*07-07-2022*	*KAI07 A*	*157*	*42.983133*	*78.465143*	*lying*	*1913*	***1958***	5	*1889*		*Recent*
8	07-07-2022	KAI08 A	113	42.980543	78.465819	lying	Undated					
9	09-07-2022	KAI09 A	75	42.984541	78.46488	lying	1845	**1887**		1830	59	
10	09-07-2022	KAI10 A	75	42.984541	78.46488	lying	1765	**1863**	1	1754	135	
11	09-07-2022	KAI11 A	63	42.984541	78.46488	lying	1783	**1887**	1	1772	117	
12	09-07-2022	KAI12 A	85	42.984541	78.46488	lying	1763	**1875**	5	1748	141	
13	09-07-2022	KAI13 A	93	42.986512	78.465434	lying	1746	**1882**	0	1736	153	
14	09-07-2022	KAI14 A		42.986512	78.465434	lying	1756	**1880**	16	1730	159	
15	*09-07-2022*	*KAI15 A*	*97*	*42.986512*	*78.465434*	lying	*1833*	***1982***		*1822*		*Recent*
16	09-07-2022	KAI16 A	144	42.986512	78.465434	lying	1755	**1885**	65	1680	209	
17	09-07-2022	KAI17 A	122	42.986512	78.465434	lying	1746	**1882**	6	1730	159	
18	09-07-2022	KAI18 AB	135	42.986512	78.465434	lying	1788	**1885**	70	1708	181	
19	*09-07-2022*	*KAI19 A*	*80*	*42.986512*	*78.465434*	*lying*	*1965*	***2014***		*1950*		*Recent*

Table 2 (continued)

	Sampling date	Tree label	Circumference (cm)	GPS LAT	GPS LONG	Position	Tree-ring serie		Number of rings between the pith and the start of the tree-ring serie (estimation)	Germination date (estimation)	Lifetime (estimation) yesrs	Remark
							Date begin	Date end				
20	09-07-2022	KAI20 AB	179	42.981952	78.464259	In situ, erected	1790	**1881**	85	1695	194	
21	09-07-2022	KAI21 A	261	42.981952	78.464259	In situ, erected	1837	**1882**	140	1687	202	
22	09-07-2022	KAI22 AB	100	42.981952	78.464259	In situ, erected	1871	**1884**	21	1840	49	
23	09-07-2022	KAI23 AB	164	42.981503	78.464483	In situ, erected	1840	**1888**	97	1733	156	
24	09-07-2022	KAI25 AB		42.981504	78.464484	In situ, erected	1786	**1883**	15	1761	128	
25	01-10-2015	KM1 A		Upper part of the lake		In situ, erected	1744	**1872**	14	1720	169	
26	01-10-2015	KM2 A		Upper part of the lake		In situ, erected	1720	**1887**	0	1710	179	
27	01-10-2015	KM3 A		Upper part of the lake		In situ, erected	1717	**1874**	1	1706	183	
28	01-10-2015	KM4 A		Upper part of the lake		In situ, erected	1724	**1880**	1	1713	176	
29	01-10-2015	KM5 A		Upper part of the lake		In situ, erected	1836	**1888**	0	1826	63	
30	01-10-2015	KM6 A		Upper part of the lake		In situ, erected	1848	**1882**	18	1820	69	
31	01-10-2015	KM7 A		Upper part of the lake		In situ, erected	1800	**1870**	10	1780	109	
32	01-10-2015	KM9 A		Upper part of the lake		In situ, erected	Undated					

Trees sampled by Akkemik et al 2022

Table 2 (continued)

	Sampling date	Tree label	Circumference (cm)	GPS LAT	GPS LONG	Position	Tree-ring serie		Number of rings between the pith and the start of the tree-ring serie (estimation)	Germination date (estimation)	Lifetime (estimation) yesrs	Remark
							Date begin	Date end				
1	11-07-2022	KAG2	101	Upper part of the lake		In situ, erected	1753	**1882**		1775	107	*Revised*
2	11-07-2022	KAG3		Upper part of the lake		In situ, erected	–	–		–	–	*Excluded*
3	11-07-2022	KAG4	94	Upper part of the lake		Lying	1815	**1871**		1810	61	
4	11-07-2022	KAG5	69	Upper part of the lake		Lying	1803	**1876**		1798	66	
5	11-07-2022	KAG6	70	Upper part of the lake		In situ, erected	–	–		–	–	*Excluded*
6	11-07-2022	KAG7	69	Upper part of the lake		Lying	1830	**1882**		1825	57	
7	11-07-2022	KAG8	144	Upper part of the lake		Lying	1786	**1862**		1740	122	
8	11-07-2022	KAG9	201	Upper part of the lake		In situ, erected	1743	**1882**		1735	147	*Revised*
9	11-07-2022	KAG10	130	Upper part of the lake		In situ, erected	1812	**1885**		1770	115	

Trees with two cores are labeled ’AB’ and those with one core are labeled ’A’

The mean chronology of drowned trees KAIDead is dated using living trees KAILife at 1717 A.D.–1888 A.D. This dendro-match is supported by various test values (Glk: 71, tvBP: 4.1, tvH: 4.5, CDI: 23) although the overlap between the two mean chronologies is rather short with only 71 years (Fig. 7a, b). Therefore, we compared the mean chronology KAIDead with seven mean site chronologies from the Tian Shan mountains available in the International Tree ring Data Bank (Grissino-Mayer and Fritts 1997) (Table 3). KAIDead showed very high correlations with the reference chronologies from Ulken and Koeliu (PAGES 2k Consortium 2013), from Qiaxi, Jialepake and Big Kishitai (Cook et al 2010), from Tschongskys (Schweingruber 2002a) and Karabatkak (Schweingruber 2002b) with CDI up to 62, Glk > 60 and very high tvBP and tvH all supporting the dating of KAIDead at 1717 AD–1888 AD (Fig. 7b).

These new data led us to correct the date of dead trees given in the study conducted by Akkemik et al. (2022). In this previous paper, the standard mean chronology (KAG) built from dead trees was initially dated to 1912 A.D. with significant statistical results (Glk, TVB, TVBP and CDI of 74%, 7.9, 9.7 and 57, respectively). Now the higher number of samples and measurements improves the quality of the replication and the reliability of crossdating. Therefore, the previously given dates must be updated: the last rings of KAG2 and KAG9 which were dated to 1912 A.D. are now dated to 1882 A.D. (Table 2). KAG3 and KAG6 which were previously dated to 1912 A.D. and 1911 A.D. were excluded in this study. We kept the other dead tree samples (KAG4, KAG5, KAG7, KAG8 and KAG10). This dating problem probably results from attempts to crossdate the outer rings of old trees with the juvenile rings of the living trees with short overlapping between compared mean chronologies.

5 Discussions

5.1 Onset and dating of the Kaindy lake

The sunken Kaindy forest was composed of ~ 143 year old trees (max: 209 years; min: 49 years) which started growing around 1680–1750 AD. This ancient forest probably looked like the *Picea* stand that today covers the slopes of the Kaindy valley; these trees are *ca*. 138 are 138 years old (max: 204 years; min: 90 years). We assess that the trees were suddenly submerged when the landslide was triggered and dammed the Kaindy river, with a lake formed upstream. We assume that, in the flooding area, all the trees drowned and died during the same event because *Picea schrenkiana* cannot survive if their roots are in submerged conditions. Most of tree species are intolerant of flooding. Flooding causes direct damage to trees by changing soil conditions, reducing the supply of oxygen to roots which must have oxygen to survive and grow, and modifying carbon dioxide exchange between trees and their environment (Kozlowski 1982).

At Kaindy Lake, we can also infer that the valley was rapidly flooded and that the *Picea* forest was suddenly submerged. Indeed, the potential volume of the Kaindy lake from the aerial view of the satellite image can be estimated to *ca*. 2 millions m^3; considering the size of the catchment of ~ 50 km^2, the mean annual precipitation (400 mm), and a given 50% runoff ratio, the annual water inflow into the lake is estimated at 10 million m^3. This is five times larger than the lake's total volume. Therefore, it can be inferred that Kaindy Lake was formed and reached a high water level (as seen in Fig. 3) within a few months after the landslide, which is also consistent with the excellent preservation state of the wood. This

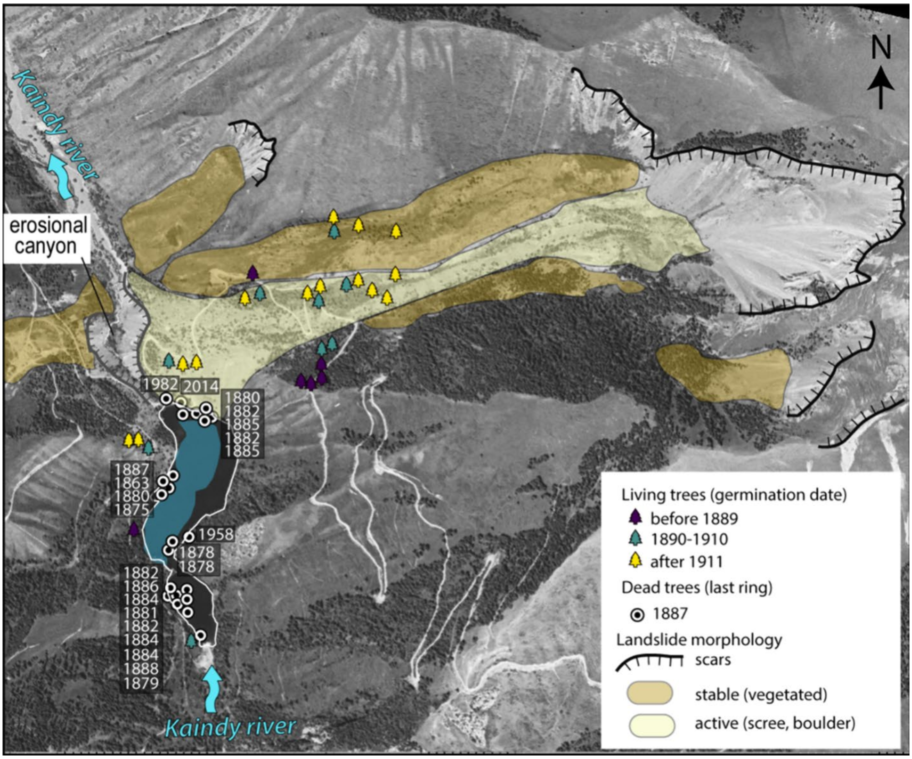

Fig. 5 Kaindy landslide morphology, and locations of sampled trees in 2022 on top of a declassified satellite image taken in 1976 (data available at https://earthexplorer.usgs.gov). The contour of Kaindy Lake in 1976 is in a light-blue line while the present-day level is represented by the dark-blue polygon. Dates of last rings for dead trees are reported in A.D. in the boxes

scenario is similar to those that have already taken place in the Cascadia Subduction Zone (Pacific Northwest coast of the U.S.) where trees died immediately after lake formations following landslides triggered by earthquakes (Atwater et al. 2005; Atwater and Yamaguchi 1991; Yamaguchi et al. 1997; Jacoby et al. 1992, 1997; Struble et al. 2020, 2021).

Moreover, our results show that 65% of the trees from the KAIDead chronology (sunken trees) have their last measured ring dated between 1882 and 1888 A.D., and we therefore propose that the lake was formed shortly after 1888 A.D. During our sampling campaign, we noticed that some trees still had some bark attached at the base of the trunk, but not higher up where we managed to collect the core samples. From this field observation, we propose that the wood decay is not significant and that the dates of the outermost preserved rings are close to their actual death.

5.2 Landslide age

Our results show that the trees collected on stable and active parts of the landslide were all established after the drowned dead trees. Extrapolated germination dates, ranging from 1898 to 1935 A.D., suggest that the landslide was set up before 1898 A.D., aligning with the formation of the landslide shortly after the 1889 A.D. earthquake. The time

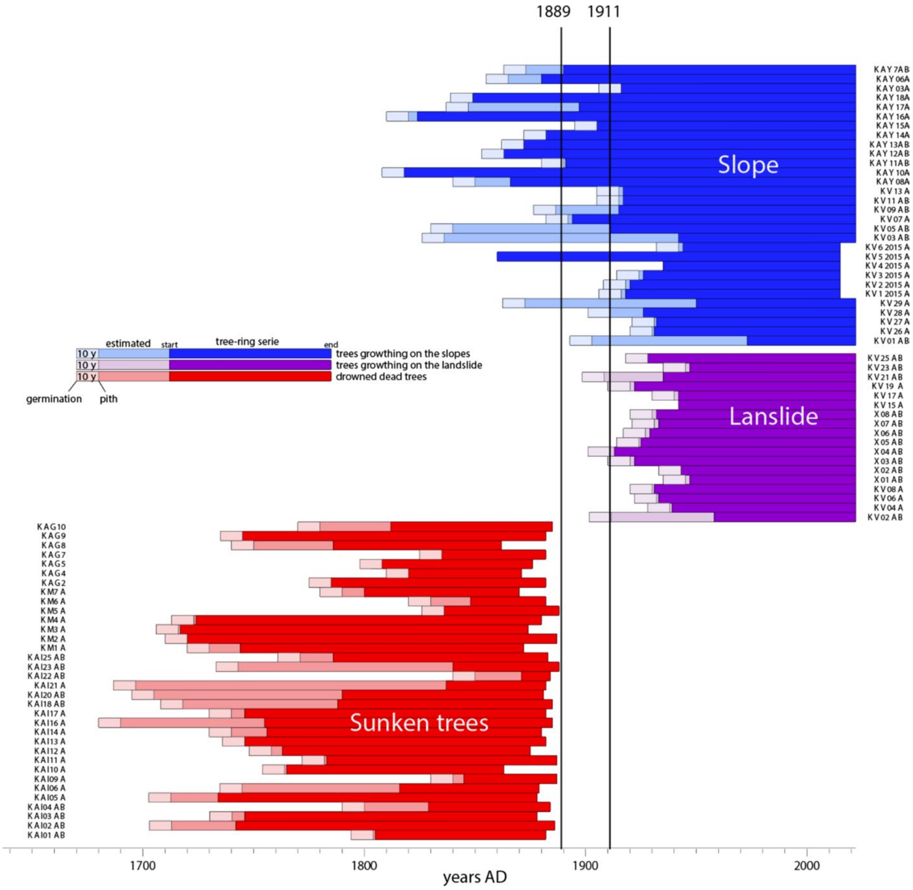

Fig. 6 Bar diagram of cross-dated ring-width series

lag between landslide and tree establishment on site is variable and depends upon substrate suitability, topography, water availability, microclimate, and seed source. The first rings of the tree X04 AB growing on the landslide, in two cores taken at breast height, were formed in 1913 A.D. supporting an estimated germination year of 1901 A.D. (Table 2, Fig. 6). This finding effectively eliminates the possibility of a 1911 landslide event. In addition, the trees collected on the left and right slopes near the landslide provide establishment dates that are older than 1888 A.D., indicating that the slopes were already vegetated and that a forest was already in place. Taken together, this dataset is consistent with the proposed age of 1889 A.D. for the lake emplacement.

5.3 Links between landslide, lake formation, and historical seismicity

To this point, the emplacement of Kaindy Lake is often associated with the triggering of a landslide-dam during the 1911 Chon-Kemin earthquake (Akkemik et al 2022,

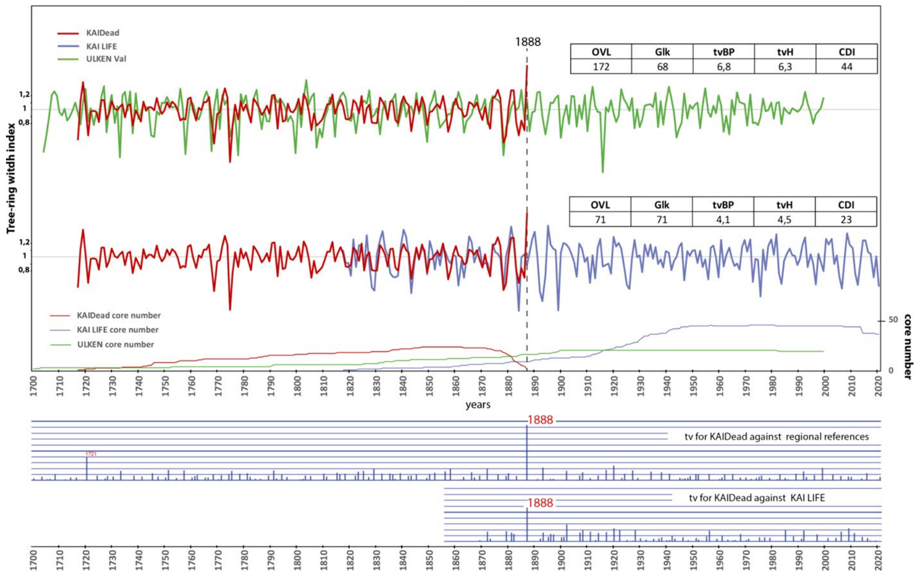

Fig. 7 Dendrochronological results **a** Visual agreement between the mean chronology KAIDead (red curve) dated to 1888 (last ring) with the reference chronologies Ulken (green one) and KAILife (blue one) **b** T value is significantly and conspicuously high for the year A.D. 1888 relative to other years

National Park brochure, Wikipedia, local lore, Guo 2019, Камендровская et Романова 2021, Виноградов 2017). Our study based on most powerful data challenges this hypothesis and by means of a thorough dendrochronological analysis brings a new scenario on the timing of the lake formation. Our data highlights that the Kaindy Lake was formed shortly after 1888 A.D. (last ring of sunken trees) and that the landslide was triggered before 1901 A.D. (first establishment estimated age on landslide). This most probable time interval therefore excludes the 1911 earthquake.

The only strong earthquake reported for the 1888–1898 A.D. period in this region is the 11 July, 1889 (M8.2) earthquake (Kalmetieva et al. 2009; Januzakov et al. 2003). Moreover, numerous slope destabilization was reported for the 1889 earthquake in the upper Chilik Valley (Bogdanovich et al. 1914), and it should be noted that the Saty River, only two valleys away from our study area, was blocked and a lake also formed (Fig. 1b). In steep topography environments, the density of earthquake-triggered landslides is usually high because the horizontal peak ground acceleration (PGA) exceeds 0.2 g, an acceleration value typically reached in regions exposed to intensities greater than VI (Meunier et al. 2007; Wald et al. 1999). The Kaindy valley is in an area with maximum local intensities reported up IX on the MSK-64 scale for the 1889 A.D. earthquake (Fig. 1; Januzakov et al. 2003; Bindi et al. 2014), that explains a high density of landslides in the Kolsay region. Moreover, the Kaindy valley is located at a distance of less than 8.5 km from the potential surface rupture of the 1889 A.D. earthquake, which is suspected within a paleoseismic trench close to the Saty village (Abdrakhmatov et al. 2016, Fig. 1b). During an earthquake, high PGA values (a landslide triggering factor) are therefore expected due to the short distance between our study area and the fault rupture zone. We then suggest that the landslide in the Kaindy valley was triggered (or re-activated) during the 1889 Chilik earthquake, damming the river, and the lake was

Table 3 Crossdating statistical values between KAIDead (1717 A.D.–1888 A.D.) and several reference chronologies from Tian Shan mountain

Site	Longitude	Latitude	OVL	Glk	tvBP	tvH	CDI
Solomina—Ulken—PCSH—ITRDB KAZ001 (1)	77.350002°	43.349999°	172	68	6.8	6.3	44
Krusic—Qiaxi—PCSH—ITRDB CHIN012 (2)	82.683300°	43.083300°	168	62	7.5	6.9	44
Krusic—Jialepake—PCSH—ITRDB CHIN009 (3)	82.150000°	43.066700°	172	67	8.4	9.2	59
Krusic—Big Kushitai—PCSH—ITRDB CHIN008 (4)	82.133300°	42.883300°	172	65	4.4	4.2	28
Solomina—Koeliu—PCSH—ITRDB KYRG012 (5)	79.049000°	42.205800°	172	60	4	4	24
Schweingruber—Tschongkys (Kirgistan)—PCSH—ITRDB RUSS164 (6)	78.180006°	42.179956°	172	70	8.6	8.9	62
Schweingruber—Karabatkak (Kirgistan)—PCSH—ITRDB RUSS156 (7)	78.180006°	42.179956°	172	69	5.6	6.1	40
KAILife (8)	78.465738°	42.984853°	71	71	4.1	4.5	23

Site	Online resource	Date accessed
1	https://www.ncei.noaa.gov/access/paleo-search/study/15230	20/02/2022
2	https://www.ncei.noaa.gov/access/paleo-search/study/12590	20/02/2022
3	https://www.ncei.noaa.gov/access/paleo-search/study/12587	20/02/2022
4	https://www.ncei.noaa.gov/access/paleo-search/study/12586	20/02/2022
5	https://www.ncei.noaa.gov/access/paleo-search/study/15237	20/02/2022
6	https://www.ncei.noaa.gov/access/paleo-search/study/4695	20/02/2022
7	https://www.ncei.noaa.gov/access/paleo-search/study/4454	20/02/2022
8	This study	

filled in a few months. Because the 1889 earthquake occurred on 11 July, only the first cells of the earlywood of the 1889-ring were formed. It thus agrees with the fact that this incomplete ring was not preserved by the sunken trees.

5.4 1889 A.D: a revised date for the lake formation

The 1889 A.D. date for the formation of Kaindy Lake contradicts common local beliefs, as well as the earlier tentative study by Akkemik et al. (2022) and also with the radiocarbon analysis conducted by V.A. Gapich on a sunken tree, dating it to 430 ± 60 BP (1406–1635 cal. A.D., 2σ) (Strom and Abdrakhmatov 2018). This radiocarbon date appears to be too old compared to the results of our study. One possible explanation is that Gapich dated the pith of a sunken tree that was more than 250–300 years old. Indeed, the innermost part of a tree trunk, composed of dead tissue, has an older radiocarbon age than the rings closer to the bark, which were formed more recently (known as the old wood effect). Unfortunately, we do not have any description of the sample collected by Gapich.

6 Conclusion

Comparing tree-ring width patterns from 32 sunken trees with 50 living trees growing on the slopes surrounding Kaindy Lake, this new dendrochronological study revises the dating of the landslide-dammed lake formation. We propose that Kaindy Lake was formed by a landslide triggered by the 1889 Chilik earthquake (M 8.2) and filled by river water within a few months. Our results also support the proposition of Abdrakhmatov et al. (2016) that the Saty fault segment ruptured during this large historical earthquake.

Dendrochronology is the most accurate dating method available for dating past geomorphological events triggered by earthquakes, such as the formation of lakes due to landslides. This method could also be applied to the neighbouring Kolsay Lakes, which are also dammed by landslides and contain submerged trees. This is possible that these lakes formed contemporaneously with Kaindy Lake. Such a study would enhance the understanding of paleoseismic activity in this region, near the city of Almaty, where earthquake hazards are significant.

The unique underwater forest of Kaindy Lake is a significant heritage site, and one of Kazakhstan's most famous tourist destinations, also included in the UNESCO World Network of Biosphere Reserves. However, the exceptional sunken trees face the risk of disappearing due to a drop in the lake's water level caused by regressive erosion, which is gradually eroding the landslide toe that dams the valley. The speed and intensity of erosion are particularly remarkable when comparing declassified satellite imagery from the 1970s with recently acquired remote sensing data. One potential solution to protect the submerged forest and prevent further lake level decline would be to construct a dam at the lake's outlet. Additionally, such a measure could help mitigate the risk of an uncontrolled dam collapse and subsequent flooding, thereby providing an added layer of safety for both the environment and local communities.

7 Supplementary information

Crossdating statistical values between KaiDead trees and T-values plot.

Supplementary Information The online version contains supplementary material available at https://doi.org/10.1007/s11069-024-06927-0.

Acknowledgements We would like to thank the support of the Institute of seismology of Kazakhstan for accompanying us in the field, and Kolsay Lakes National Park for authorizing us to take samples from the trees. We would like to thank an anonymous reviewer and Christoph Grützner for taking the time to correct our manuscript and for their pertinent comments and criticisms.

Author contributions Cécile Miramont and Magali Rizza were involved in funding acquisition, supervision, and writing. The first draft of the manuscript was written by Cécile Miramont and Magali Rizza and all authors commented on previous versions of the manuscript. All authors read and approved the final manuscript. Material preparation was performed by Cécile Miramont with the help of Paul Millagou and Eliane Charrat. Dendrochronological analysis was performed by Cécile Miramont in collaboration with Ünal Akkemik and Frédéric Guibal. Cécile Miramont, Magali Rizza, Frédéric Guibal, Elodie Brisset, Lenka Brousset, Frédéric Guiter, Satbek Sarzhanov, Baurzhan Adikhan, and Aidyn Mukambayev were involved in the fieldtrip and the sampling campaign.

Funding This work received support from the French government under the France 2030 investment plan, as part of the Initiative d'Excellence d'Aix-Marseille Université—A*MIDEX (AMX-19-IET-012) and from the Research Federation ECCOREV (FR 3098; Aix-Marseille Univ., CNRS, INRAE, IRSN, CEA, Univ. Toulon, Univ. Avignon, Univ. Nimes).

Declarations

Conflict of interest The authors have no relevant financial or non-financial interests to disclose.

References

Abdrakhmatov KE, Walker RT, Campbell GE, Carr AS, Elliott A, Hillemann CJ, Hollingsworth LA, Mackenzie D, Mukambayev A, Rizza M, Sloan RA (2016) Multisegment rupture in the 11 July 1889 Chilik earthquake (Mw 8.0–8.3), Kazakh Tien Shan, interpreted from remote sensing, field survey, and paleoseismic trenching. J Geophys Res Solid Earth 121(6):4615–4640. https://doi.org/10.1002/2015JB012763

Akkemik U, Mazarzhanova K, Kopabayeva A (2022) A case study on geomorphology: tree-ring-based confirmation of the formation year of Lake Kaindy after the 1911 Kemin earthquake in Almaty (Kazakhstan). Turk J Earth Sci 31(6):622–628. https://doi.org/10.55730/1300-0985.1823

Alestalo J (1971) Dendrochronological interpretation of geomorphic processes. Fennia Int J Geogr 105(1):1–139

Amey RMJ, Elliott JR, Hussain E, Walker R, Pagani M, Silva V, Abdrakhmatov K, Watson C (2021) Significant seismic risk potential from buried faults beneath Almaty city, Kazakhstan, revealed from high-resolution satellite DEMs. Earth Space Sci. https://doi.org/10.1029/2021EA001664

Arrowsmith JR, Crosby CJ, Korzhenkov AM, Mamyrov E, Povolotskaya I, Guralnik B, Landgraf A (2017) Surface rupture of the 1911 Kebin (Chon–Kemin) earthquake, Northern Tien Shan, Kyrgyzstan. Geol Soc Lond Spec Publ 432(1):233–253. https://doi.org/10.1144/SP432.10

Atwater BF, Satoko MR, Kenji S, Yoshinobu T, Kazue U, Yamaguchi DK (2005) The Orphan Tsunami of 1700: Japanese Clues to a Parent Earthquake in North America. USGS Prof Pap. https://doi.org/10.3133/pp1707

Atwater BF, Yamaguchi DK (1991) Sudden, probably coseismic submergence of Holocene trees and grass in coastal Washington State. Geology 19:706–709. https://doi.org/10.1130/0091-7613(1991)019%3c0706:SPCSOH%3e2.3.CO;2

Baillie MGL, Pilcher JR (1973) A simple cross-dating program for tree-ring research. Tree-Ring Bull 33:7–14

Bekker MF (2010) Tree rings and earthquakes. Wasatch dendroclimatology research. Paper 13. In: Stoffel M et al (eds) Tree rings and natural hazards. Springer, pp 391–397

Bindi D, Parolai S, Gómez-Capera A, Locati M, Kalmetyeva Z, Mikhailova N (2014) Locations and magnitudes of earthquakes in Central Asia from seismic intensity data. J Seismolog 18:1–21. https://doi.org/10.1007/s10950-013-9392-1

Black BA, Pearl JK, Pearson CL, Pringle PT, Frank DC, Page MT et al (2023) A multifault earthquake threat for the Seattle metropolitan region revealed by mass tree mortality. Sci Adv 9(39):eadh4973. https://doi.org/10.1126/sciadv.adh4973

Bogdanovitch KI, Kark IM, Korolkov BY, Musketov DL (1914) The earthquake in the northern district of the Tien shan. December 1910 (4 January 1911). Commission of the Geology Committee, Leningrad (**in Russian**)

Виноградов АВ (2017) аналитический обзор биогеографии континентальных водоёмов европы, нагорной и центральной азии. Научное Обозрение Биологические Науки 2:17–41

Carrara PE, O'Neill JM (2003) Tree-ring dated landslide movements and their relationship to seismic events in southwestern Montana, USA. Quatern Res 59(1):25–35. https://doi.org/10.1016/S0033-5894(02)00010-8

Carrara PE, O'Neill JM (2010) Tree-ring dated landslide movements and seismic events in southwestern Montana, U.S.A. In: Stoffel M, Bollschweiler M, Butler DR, Luckman BH (eds) Tree rings and natural hazards: a state-of-the-art. Springer, Berlin, pp 421–436. https://doi.org/10.1007/978-90-481-8736-2_39

Cook ER, Kairiukstis LA (1990) Methods of dendrochronology. Appl Environ Sci Int Inst Appl Syst Anal. https://doi.org/10.1007/978-94-015-7879-0

Cook ER, Anchukaitis KJ, Buckley BM, D'Arrigo RD, Jacoby GC, Wright WE (2010) Asian monsoon failure and megadrought during the last millennium. Science 328(5977):486–489. https://doi.org/10.1126/science.1185188

Deev EV, Korzhenkov AM (2016) Paleoseismological studies in the epicentral area of the 1911 Kemin earthquake (northern Tien Shan). Russ Geol Geophys 57(2):337–343

DeGraff JV, Agard SS (1984) Defining geologic hazards for natural resources management using tree-ring analysis. Env Geol Water Sci 6(3):147–155. https://doi.org/10.1007/BF02509908

Delvaux D, Abdrakhmatov KE, Lemzin IN, Strom AL (2001) Landslides and surface breaks of the 1911 Ms 8.2 Kemin earthquake. Landslides 42:1583–1592

Dziak RP, Black BA, Wei Y, Merle SG (2021) Assessing local impacts of the 1700 CE Cascadia earthquake and tsunami using tree-ring growth histories: a case study in South Beach, Oregon, USA. Nat Hazards Earth Syst Sci 21:1971–1982. https://doi.org/10.5194/nhess-21-1971-2021

Eckstein D, Bauch J (1969) Beitrag zur Rationalisierung eines dendrochronologischen Verfahrens und zur Analyse seiner Aussagesicherheit. Forstwissenschaftliches Centralblatt 88:230–250

Grissino-Mayer HD (2003) A manual and tutorial for the proper use of an increment borer. Tree-Ring Res 59:63–79

Grissino-Mayer HD, Fritts HC (1997) The International Tree-Ring Data Bank (ITRDB). IGBP PAGES/World Data Center for Paleoclimatology Data Contribution Series #1997–015. NOAA/NGDC Paleoclimatology Program, Boulder CO, USA. https://www.ncdc.noaa.gov/paleo-search/?dataTypeId=18

Guo J (2019) The application of dead trees or dying trees in landscape design. Res Ecol 1(2):24–30

Havenith HB, Strom A, Jongmans D, Abdrakhmatov K, Delvaux D et al (2003) Seismic triggering of landslides, Part A: Field evidence from the Northern Tien Shan. Nat Hazard 3:135–149. https://doi.org/10.5194/nhess-3-135-2003

Hay MB (1888) The earthquakes of May and June, 1887, in the Verny (Vernoe) District, Russian Turkestan, and their consequences. Proc R Geogr Soc Mon Rec Geogr 10:638–646. https://doi.org/10.2307/1800851

Hollstein E (1980) Mitteleuropäische Eichenchronologie. Trierer dendrochronologische Forschungen zur Archäologie und Kunstgeschichte, Trierer Grabungen u. Forsch., 11

Holmes RL (1983) Computer-assisted quality control in tree-ring dating and measurement. Tree Ring Bull 43:69–78

Jacoby GC, Shepphard PR, Sieh KE (1988) Irregular recurrence of large earthquakes along the San Andreas Fault: Evidence from Trees. Science 241(4862):196–199

Jacoby GC, Williams PL, Buckley BM (1992) Tree ring correlation between prehistoric landslides and abrupt tectonic events in Seattle, Washington. Science 258(5088):1621–1623

Jacoby GC, Bunker DE, Benson BE (1997) Tree-ring evidence for an A.D. 1700 Cascadia earthquake in Washington and northern Oregon. Geology 25:999–1002. https://doi.org/10.1130/0091-7613(1997)025%3c0999:TREFAA%3e2.3.CO;2

Januzakov K., Omuraliev M., Omuralieva A, Ilyasov B, Grebennikova V (2003). Strong earthquakes of the Tien Shan (within the Kyrgyzstan territory and adjacent regions of the countries of Central Asia). Ilim, Bishkek

Kalmetieva ZA, Mikolaichuk AV, Moldobekov BD, Meleshko AV, Jantaev MM, Zubovich AV, Havenith, HB (2009). Atlas of earthquakes in Kyrgyzstan. CAIAG, Bishkek, 76

Камендровская В А and Романова М М (2021) Проблемы и тенденции развития туризма (На Примере Казахстана). In Интеграция туризма в экономическую систему региона: перспективы и барьеры 245–253

Kozlowski TT (1982) Water supply and tree growth. Part II Flooding for Abstr 43(3):145–161

Kulikova G, Krüger F (2015) Source process of the 1911 M 8.0 Chon-Kemin earthquake: investigation results by analogue seismic records. Geophys J Int 201(3):1891–1911. https://doi.org/10.1093/gji/ggv091

Lawrence DB (1936) The submerged forest of the Columbia River Gorge. Geogr Rev 26:581–592

Lawrence DB (1937) Drowned forests of the Columbia River Gorge. Geol Soc Oregon Country Newslett 3:78–83

Maxwell RS, Larsson LA (2021) Measuring tree-ring widths using the CooRecorder software application. Dendrochronologia 67:125841. https://doi.org/10.1016/j.dendro.2021.125841

Meunier P, Hovius N, Haines AJ (2007) Regional patterns of earthquake-triggered landslides and their relation to ground motion. Geophys Res Lett 34(20):L20408. https://doi.org/10.1029/2007GL031337

Mushketov IV (1891) Materials for studying earthquakes In Russia. Izvestiia Russkogo geograficheskogo. Issue 1 (Supplement to vol. 27 of Proceedings of the Imperial Russian Geographical Society). Printing House of A.S. Suvorin, St.-Petersburg, 62p. (**in Russian**)

Owczarek P, Opała-Owczarek M, Rahmonov O, Mendecki M (2017) 100 years of earthquakes in the Pamir region as recorded in juniper wood: a case study of Tajikistan. J Asian Earth Sci 138:173–185. https://doi.org/10.1016/j.jseaes.2017.02.011

PAGES 2k Consortium (2013) Continental-scale temperature variability during the past two millennia. Nat Geosci 6:339–346. https://doi.org/10.1038/NGEO1797

Peel MC, Finlayson BL, Mcmahon PA (2007) Updated world map of the KöppenGeiger climate classification. Hydrol Earth Syst Sci 4:439–473. https://doi.org/10.5194/hess-11-1633-2007

Pirie MR, Fowler AM, Triggs CM (2015) Assessing the accuracy of three commonly used pith offset methods applied to Agathis australis (Kauri) incremental cores. Dendrochronologia 36:60–68. https://doi.org/10.1016/j.dendro.2015.10.003

Rinn F (1991–2023) TSAP - Software for Times Series Analysis and Presentation. RINNTECH, Heidelberg/Germany, 110 p

Russian Meteorological Agency (2023) Погода и климат Weather and climate http://www.pogodaiklimat.ru/history/36897.htm. Accessed 4 Sept 2024

Schweingruber FH (2002a) NOAA/WDS Paleoclimatology - Schweingruber - Tschongkys (Kirgistan) - PCSH - ITRDB RUSS164. NOAA National Centers for Environmental Information. https://doi.org/10.25921/19rd-a209. Accessed 05 Sept 2024

Schweingruber FH (2002b) NOAA/WDS Paleoclimatology - Schweingruber - Karabatkak (Kirgistan) - PCSH - ITRDB RUSS156.. NOAA National Centers for Environmental Information. https://doi.org/10.25921/5nbc-sm14. Accessed 05 Sept 2024

Sheppard PR, Jacoby GC (1989) Application of tree-ring analysis to paleoseismology: two case studies. Geology 17:226–229. https://doi.org/10.1029/96RG03526

Sloan RA, Jackson JA, McKenzie D, Priestley K (2011) Earthquake depth distributions in central Asia, and their relations with lithosphere thickness, shortening and extension. Geophys J Int 185(1):1–29. https://doi.org/10.1111/j.1365-246X.2010.04882.x

Speer J (2010) Fundamentals of tree ring research. University of Arizona Press, Arizona

Stoffel M, Bollschweiler M (2008) Tree-ring analysis in natural hazards research: an overview. Nat Hazards Earth Syst Sci 8:187–202. https://doi.org/10.5194/nhess-8-187-2008

Strom A, Abdrakhmatov K (2018) Rockslides and rock avalanches of Central Asia, distribution, morphology, and internal structure. Elsevier, p 418

Strom AL, Korup O (2006) Extremely large rockslides and rock avalanches in the Tien Shan Mountains, Kyrgyzstan. Landslides 3(2):125–136. https://doi.org/10.1007/s10346-005-0027-7

Struble WT, Roering JJ, Black BA, Burns WJ, Calhoun N, Wetherell L (2020) Dendrochronological dating of landslides in western Oregon: eearching for signals of the Cascadia A.D. 1700 earthquake. Geol Soc Am Bull 132(7–8):1775–1791. https://doi.org/10.1130/B35269.1

Struble WT, Roering JJ, Burns WJ, Calhoun NC, Wetherell LR, Black BA (2021) The preservation of climate-driven landslide dams in western Oregon. J Geophys Res Earth Surf 126(4):e2020JF005908. https://doi.org/10.1029/2020JF005908

Tatevossian RE (2007) The Verny, 1887, earthquake in Central Asia: application of the INQUA scale, based on coseismic environmental effects. Quatern Int 173:23–29

Tapponnier P, Molnar P (1979) Active faulting and Cenozoic tectonics of the Tien Shan, Mongolia, and Baykal regions. J Geophys Res Solid Earth 84(B7):3425–3459. https://doi.org/10.1029/JB084iB07p03425

Tibaldi A, Graziotto E, Forcella F, Gapich VH (1997) Morphotectonic indicators of Holocene faulting in central Tien Shan, Kazakstan, and geodynamic implications. J Geodyn 23(1):23–45. https://doi.org/10.1016/S0264-3707(96)00021-X

Wald DJ, Quitoriano V, Heaton TH, Kanamori H (1999) Relationships between peak ground acceleration, peak ground velocity, and modified Mercalli intensity in California. Earthq Spectra 15(3):557–564

Yamaguchi DK, Atwater BF, Bunker DE, Benson BE, Reid MS (1997) Tree-ring dating the 1700 Cascadia earthquake. Nature 389(6654):922–923. https://doi.org/10.1038/40048

Publisher's Note Springer Nature remains neutral with regard to jurisdictional claims in published maps and institutional affiliations.

Authors and Affiliations

Cécile Miramont[1] · Magali Rizza[2,7] · Frédéric Guibal[1] · Elodie Brisset[1] · Lenka Brousset[1] · Frédéric Guiter[1] · Paul Millagou[1] · Satbek Sarzhanov[3] · Baurzhan Adilkhan[3] · Ünal Akkemik[4] · Kuralay Mazarzhanova[5] · Arailym Kopabayev[5] · Aidyn Mukambayev[6]

✉ Cécile Miramont
cecile.miramont@imbe.fr

[1] CNRS, IRD, IMBE, Aix Marseille Univ, Avignon Univ, Marseille, France

[2] CNRS, IRD, Coll. France, INRAE, CEREGE, Aix Marseille Univ., Aix-en-Provence, France

[3] Institute of Seismology of Kazakhstan, Almaty, Kazakhstan

[4] Department of Forest Botany, Faculty of Forestry, İstanbul University-Cerrahpasa, Bahçeköy, İstanbul, Turkey

[5] Department of Forest Resources and Forestry, Faculty of Forestry, Wildlife and Environment, S. Seifullin Kazakh Agrotechnical University, Nur-Sultan, Kazakhstan

[6] National Nuclear Center of the Republic of Kazakhstan, Kurchatov, Kazakhstan

[7] Université du Québec, Département des sciences de la terre et de l′atmosphère, Montréal, Canada